Spreading and accumulation of river-borne sediments in the coastal ocean after the environmental disaster at the Doce River in Brazil

Angelo T. Lemos[1,*] , Alexander Osadchiev[2,3] , Piero L. F. Mazzini[4] , Guilherme N. Mill[5] , Sabrina A. R. Fonseca[5] , Renato D. Ghisolfi[5]

[1] Universidade Federal do Sul da Bahia - Centro de Formação em Ciências Ambientais - Campus Sosígenes Costa (Rodovia Joel Mares, BR 367 - Km 10, s/n - Porto Seguro - 45.810-000 - BA - Brazil)

[2] Russian Academy of Sciences - Shirshov Institute of Oceanology (Nakhimovskiy Ave, 36, Moscow, 117218 - Russia)

[3] Moscow Institute of Physics and Technology (Dolgoprudny, Moscow Region, 141701, Russian Federation)

[4] Virginia Institute of Marine Science, William & Mary (1370 Great Rd, Gloucester Point, VA 23062, USA)

[5] Universidade Federal do Espírito Santo - Departamento de Oceanografia e Ecologia (Av. Fernando Ferrari, 514 - Campus de Goiabeiras - Vitória - 29075-910 - ES - Brazil)

* Corresponding author: angelolemos@ufsb.edu.br

ABSTRACT

This study is focused on the fate of a large volume of mine slurry discharged from the Doce River (DR) to the coastal ocean after the worst environmental disaster in Brazilian which occurred in November 2015. We used Eulerian (ROMS) and Lagrangian (STRiPE) numerical models, as well as satellite remote sensing data, to study the spreading and seafloor accumulation of fine river-borne sediments during the initial six months following the disaster. We show that the regions of intense sediment accumulation were determined by spreading patterns of the surface-advected DR plume. The river discharge rate governed the plume surface area, while its position depended on local wind forcing conditions. The spreading of sediments carried by the DR plume was dominated by southward transport caused by prevailing upwelling-favorable northeasterly winds during the study period. Under high discharge conditions, river-borne sediments were transported over 100 km southward from the DR mouth and reached the outer shelf. In contrast, sediments were arrested near the mouth during drought periods and remained on the inner shelf. As a result, fine river-borne sediments accumulated on the seafloor, mainly in the large shallow shelf area southward from the DR mouth. Conversely, only a small fraction of residue was deposited northward. Thus, the Environmental Protection Area (EPA) of Costa das Algas, located 40 km southward from the DR, potentially exhibited more susceptibility to sediment arrival. On the other hand, their influence on Abrolhos Marine National Park, located 200 km northeastward from the DR mouth, was presumably minimal.

Descriptors: River plume, Modeling, Stripe, Roms, Wind-driven.

INTRODUCTION

Buoyant river plumes are typical coastal features transitioning the continental runoff into shelf waters. These surface-advected sub-mesoscale and mesoscale structures are generally characterized by, first, more intense motion in response to external forcing as compared to ambient coastal circulation and, second, stronger stratification that leads to reduced mixing between the surface layer and deeper waters (Garvine, 1984; Garvine, 1995; Cole and Hetland, 2015; Mazzini and Chant, 2016; Fisher et al., 2018; Mazzini et al., 2019). As a result, buoyant river plumes can effectively transport large volumes of freshwater, terrigenous sediments, nutrients, carbon, litter, and anthropogenic pollutants from tens to hundreds

of kilometers away from the river mouths. Hence, they influence water quality, bottom morphology, biological productivity, and food webs in broad coastal areas (Wright, 1977; Milliman and Syvitski, 1992; Jickells, 1998; Rabalais et al., 2002; Wang, 2006; Reifel et al., 2009; Borges and Gyphens, 2010). As just stated, river water can contain suspended and/or dissolved toxic pollutants (e.g., heavy metals, persistent organic pollutants, pesticides, plastic litter) which are discharged to the sea and are transported by river plumes. In this case, risk assessment of the negative impact of river discharge on coastal environments is based on the identification of transport pathways and accumulation areas of river-borne pollutants (Wen et al., 1999; Beusen et al., 2005; Milliman and Farnsworth, 2011).

The shape, size, and spread of a river plume are determined by river discharge rate, local winds, waves, tides, ambient currents, local bathymetry, and Coriolis force (Chant, 2011). However, the structure and dynamics of river plumes vary in space and time, mainly when formed by small and medium-size rivers (Osadchiev, 2015; Osadchiev and Korshenko, 2017; Osadchiev and Sedakov, 2019). As a result, the large daily and synoptic variability of river plumes hinders the precise reconstruction of their three-dimensional structure using in situ measurements. In this work, we combine satellite data with numerical modeling to study the fate of river-borne sediments discharged into the coastal ocean as a consequence of the worst environmental disaster in Brazilian history, the 2015 dam collapse in Mariana, Minas Gerais State (MG) (Escobar, 2015; Carmo et al., 2017).

REGIONAL SETTING

The Doce River (DR) is one of the largest rivers in southeastern Brazil. Its drainage basin area exceeds 83,000 km² (Aprile et al., 2004), 98% of which is located within the Atlantic Forest characterized by endemism and human interventions (Myers et al., 2000), which caused strong anthropogenic pressure before the Fundão dam collapse (Gomes et al., 2017). In due course, more than 200 municipalities with a total population exceeding 2 million inhabitants are located in the DR basin, and a large volume of untreated sewage is discharged into the river (ANA, 2016).

The river mouth is situated in the municipality of Regência, Linhares, Espírito Santo (ES) (19.6°S, 39.8°W), discharging approximately 500 m³ s⁻¹ on average of fresh-water into the continental shelf. The DR basin is located in the wet tropical climate zone, where the air temperature is commonly above 18°C and the mean precipitation rate is approximately 1,200 mm year⁻¹ (Guimarães et al., 2010). The rainy period occurs between October – March, with a maximum in January. As a result, the annual hydrograph of the DR is characterized by summer-autumn freshet (1,200 m³ s⁻¹) and winter-spring draught (250-300 m³ s⁻¹), with periods of regular flash floods (exceeding 5,000 m³ s⁻¹) caused by active precipitation events (Lima et al., 2010; Oliveira and Quaresma, 2017; Hatje et al., 2017).

The ES continental shelf is shallow (typically less than 60 m deep) and narrow (approximately 45 km wide). A wider continental shelf is present in southern Bahia (BA, Figure 1) (approximately 190 km wide). The upper 200 m of the water column in this region (also outside the continental shelf) is composed of Tropical Water (TW), with temperature and salinity of 20°C and 36, respectively (Emilsson, 1961; Miranda, 1985; Castro et al., 2006). Colder (T < 20°C) and more saline (S < 36.4) South Atlantic Central Water (SACW) is located beneath the TW and is associated with the upper part of the permanent thermocline (Castro and Miranda, 1998). The vertical structure of the continental shelf is governed by mixing between TW and SACW on its outer shelf and between the continental discharge and TW on its inner shelf (Castro and Miranda, 1998; Stramma and England, 1999).

Circulation in the study area is governed by the Brazil Current (BC), a southward western boundary current of the Subtropical Gyre in the South Atlantic Ocean (Peterson and Stramma, 1991), and winds driving coastal currents in shallow waters. Interaction of the BC with local bathymetry and topographic features results in eddy formation, meanders, and bottom intrusions of SACW along with the shelf break and at seamount edges
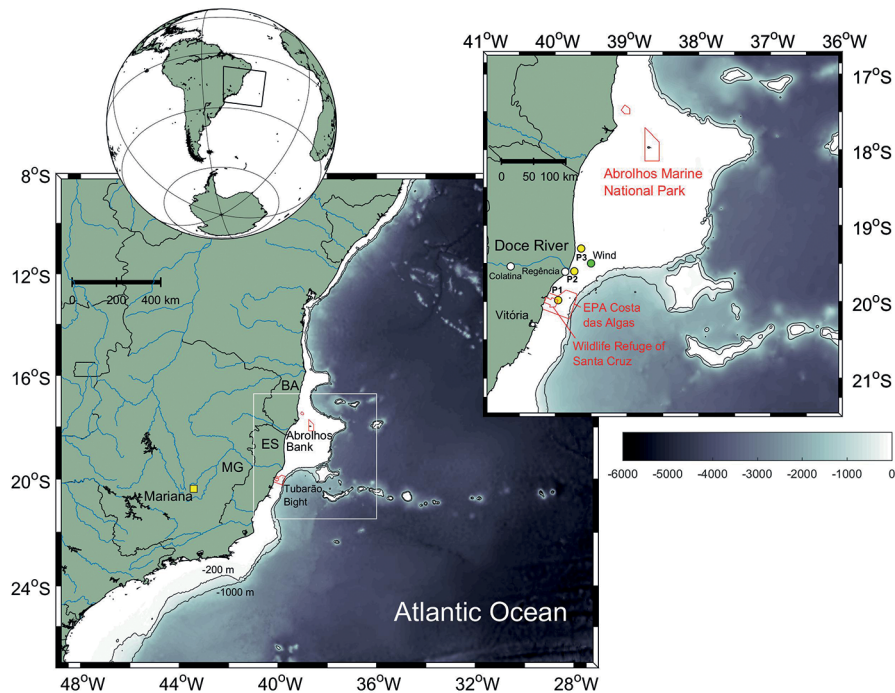
Figure 1. Left: Study area at the central part of the Brazilian coast (the coarse grid domain of numerical modeling). Right: Continental shelf of Espírito Santo State (ES) and south of Bahia State (BA) limited by the 200 m isobath (the fine grid domain of numerical modeling) and locations of EPA Costa das Algas (southern red polygon) and the Abrolhos Marine National Park (northern red polygon). The green circle represents the point where daily wind data from European Centre for Medium-Range Weather Forecasts (ERA-Interim/ECMWF) were obtained, while the yellow points represent the location of the three bottom-mounted ADCPs, used to validate the ROMS experiment.

(Ekau, 1999; Arruda et al., 2013; Soutelino et al., 2013). The intensity of cold and nutrient-rich up-welled SACW along the continental shelf is governed by wind forcing (e.g., Castelão and Barth, 2006; Mazzini and Barth, 2013), flow-topography interactions (Rodrigues and Lorenzzetti, 2001; Mazzini and Barth, 2013), and interaction with the BC (e.g., Paloczy et al., 2016).

Environmental protected areas

The river mouth of the DR is located approximately 200 km away from the Abrolhos Marine National Park, which has the most extensive and richest coral reef area in the southwestern Atlantic Ocean (Leão and Kikuchi, 2005). This national park is located off the coast of southern BA (Francini-Filho et al., 2008) (upper red polygon in Figure 1), covering an area of 913 km². The coral reefs of the Abrolhos Marine National Park are significantly different from most coral reefs globally,

with many endemic and archaic coral species originating from the Tertiary Age species, and adapted to the high turbidity waters of the Brazilian shelf (Leão, 1999).

The other two relevant conservation units located approximately 40 km southward from the DR mouth are the Environmental Protection Area Costa das Algas (EPA Costa das Algas, red polygon close to Vitória city in Figure 1) and the Wildlife Refuge of Santa Cruz (http://www.icmbio. gov.br/portal/). The EPA Costa das Algas covers 1,149.31 km² of the continental shelf of ES, from the coastline to the shelfbreak at the 700 m iso-bath. A large variety of ocean life is found in the EPA Costa das Algas, with the predominant occurrence of biotritic and biolitoclastic sediments and lateritic breastplates, and lithoclast sediments. Also, this area is characterized by a variety of marine macroalgae, calcareous and non-calcareous, non-limestone, edible and articulated macroalgae

that provide substrate, shelter, and feeding for diverse benthic, demersal, and pelagic fauna in the region (IBAMA, 2006).

2015 Dam Collapse in Mariana, Minas Gerais State, Brazil

This work addresses the worst environmental disaster in Brazilian history. The Fundão iron mine dam collapsed in the municipality of Mariana, MG (Figure 1) on November 5, 2015, releasing over 43 million m^3 of exposed mine tailing wastes directly into the DR watershed (Samarco, 2016). The mine slurry was then transported approximately 663 km along the DR through the states of MG and ES. Sixteen days following the disaster (i.e. November 21, 2015), water and sediments from the DR began entering the coastal ocean. Suspended sediments detected in the DR estuary were dominated by a fine fraction (1-200 m) with high SiO_2, Fe, Mn, Ca, and Cr (Segura et al., 2016; Gomes et al., 2017) concentrations.

After the disaster, the field surveys performed on the continental shelf near the DR mouth focused on evaluating the potential impact on the marine environment of harmful suspended and dissolved pollutants carried by the DR plume (Bianchini, 2016; Fernandes et al., 2016). However, few numerical modeling studies have been conducted to investigate the spreading and settling of suspended sediments along the coast during the first few months following the introduction of mine tailing waste into the ocean (Marta-Almeida et al., 2016; Magris et al., 2019). Also, this work intends to contribute to the investigation of the potential environmental impact on susceptible coral reefs of Abrolhos Marine National Park. The accumulation of river-borne pollutants in this area could negatively affect coral growth, photosynthesis, and respiration and, thus, lead to a decrease in the diversity of local coral species (Coles and Jokiel, 1992; Woesik et al., 1995; Woesik et al., 1999; Fabricius, 2005; Burke, 2011; Berkelmans et al., 2012; Erftemeijer et al., 2012).

This study reconstructed the transport and deposition of river-borne sediments based on satellite imagery and numerical modeling. We addressed three main questions: (1) What are the spreading patterns of the surface-advected plume formed by the Doce River and how are they impacted by wind forcing and discharge magnitude? (2) Did fine suspended mine slurry decant and accumulate on the continental shelf, or was it transported offshore? (3) Did river-borne sediment reach Abrolhos Marine National Park and/or EPA Costa das Algas and deliver suspended mine tailing waste?

METHODS

This study focuses on the spreading and accumulation of river-borne sediment discharged from the DR during the six months (November 2015 to April 2016) after the environmental disaster. We chose this period because the dam breach remained an important source of suspended particulate material even three months after the disaster (Hatje et al., 2017), and because the maximum annual precipitation in the study region occurs in January (Guimarães et al., 2010).

River discharge, wind stress, and current data

Daily DR discharge data came from the most downstream operational gauge station (ID: 56994510, http://www.snirh.gov.br/hidroweb/, approximately 110 km upstream from the river mouth) located in Colatina city (Figure 1). The available discharge data covers the period from 1990 to 2016. Based on this data, we calculated monthly mean and standard deviation values for this period and monthly means between October 2015 and December 2016.

Wind results used in the study region originated from the ERA-Interim/ECMWF dataset (Dee et al., 2011). Calculated wind stress estimates were based on Large and Pond's (1981) formulation for the grid point located closest to the river mouth (green circle in Figure 1).

Direct observations of currents and sea surface height (SSH) used in this study were obtained by three bottom-mounted ADCPs (Nortek Signature 1000 kHz) located along the 17 m-isobath (yellow circle in Figure 1). We analyzed hourly averages of the data collected every 20 minutes with a vertical resolution of 0.2 m during January 2019. Gaps associated with equipment malfunction represented less than 1% of the observations, so gaps smaller than 6-h were linearly interpolated.

Satellite Remote Sensing

The spread of the DR plume was investigated using Level-2 MODIS-Terra and MODIS-Aqua imagery data collected between 2013-2018, downloaded from the NASA website (http://oceancolor.gsfc.nasa.gov).

Ocean circulation model

The Regional Ocean Modeling System (ROMS) (Shchepetkin and McWilliams, 2005; Haidvogel et al., 2008) was used to simulate the ocean circulation of the study region between 2015-2016. Here we extended our numerical simulation until January 2019 due to the lack of in situ measurements in the study region at the referred time. ROMS is a three-dimensional, free-surface, terrain-following model that solves the Reynolds-averaged Navier-Stokes equations using hydrostatic and Boussinesq approximations. Two regular horizontal grids were implemented for the study area, namely, a coarse grid (49°W-27°W and 27°S-8°S, on the left in Figure 1) and a finer grid (41°W-36.4°W and 21.5°S-16.7°S) (on the right in Figure 1) with approximately 4.6 km and 900 m spatial and horizontal mean resolution, respectively. Both grids have closed western boundaries but opened eastern, southern, and northern boundaries.

The vertical coordinate has 40 s-levels irregularly spaced to provide higher resolution near the surface. The bathymetric data came from the General Bathymetric Chart of the Oceans (GEBCO) with 30 arc-second spatial resolution (IOC et al., 2003). Surface forcing conditions include wind, humidity, pressure, air temperature, precipitation, and radiation data obtained from ERA-Interim/ECMWF (Dee et al., 2011), with 3-hour temporal resolution and 79 km of spatial resolution. Tidal forcing was obtained from the TPXO 9.0 global database (Egbert and Erofeeva, 2002), which provided amplitudes and phases of the ten major tidal harmonic constituents with a spatial resolution of $1/4°$ $1/4°$, used at the open boundaries of the coarse grid (M_2, S_2, N_2, K_2, K_2, O_1, P_1, Q_1, M_f and M_m). The HYbrid Coordinate Ocean Model (HYCOM Global 1/12°, approximately 9.5 km of horizontal resolution) coupled with the Navy Coupled Ocean Data Assimilation (NCODA) system reanalysis (HYCOM, 2011) provided the initial and daily boundary conditions (temperature, salinity, elevation, and velocities).

Sediment model

A Lagrangian particle-tracking module simulated the transport and settling of fine suspended sediments discharged from the DR. Both horizontal and vertical sediment particle movements were calculated using deterministic and stochastic components. The former is defined by the motion of ambient water and sinking of a particle under the gravitational force, whereas the latter is a stochastic random-walk scheme that reproduces the influence of small-scale turbulent mixing. Particles initially released from the river mouth have their horizontal transport determined by the internal dynamics of a river plume simulated by the Surface-Trapped River Plume Evolution model (STRiPE). After the sediment particle settles beneath the plume, its movement is governed by the ambient coastal circulation, reproduced by the ROMS model. A similar configuration of coupled Eulerian and Lagrangian models was recently used for the simulation of the delivery and fate of terrigenous sediments discharged by the Peinan River at the southeastern coast of Taiwan (Korotenko et al., 2014; Osadchiev et al., 2016) and by numerous small river plumes located at the northeastern coast of the Black Sea (Osadchiev and Korshenko, 2017).

The STRiPE module was forced by wind forcing from ERA Interim/ECMWF (Dee et al., 2011) and coastal circulation provided by ROMS output. The particles released at the coastline close to the river mouth have outflow velocities computed using river discharge data from National Water Agency (ANA) (SNIRH, 2017) considering the river mouth width of 150 m and depth of 5 m. Total suspended matter concentrations in the DR water were prescribed according to weekly in situ data collected in the Colatina city station between October 2015 and April 2016 by the "Companhia de Pesquisa de Recursos Minerais" (CPRM 2015), whereas the sediment grain size distribution was set based on in situ measurements performed in the DR mouth before the environmental disaster (Aprile et al., 2004). The time series of turbidity (NTU) and total dissolved solids (mg L^{-1}) of the DR obtained from

CPRM in Colatina station are shown in Figure 2. We use the sediment discharge (kg s^{-1}) (blue line in Figure 2) in the sediment model, calculated considering the total dissolved solids and the river discharge. This study focuses on relatively small particles (clay and colloidal fraction) with diameters less than 10^{-6} m, which are generally transported far from the river mouth and are dispersed over a vast coastal area due to their low gravitational settling velocity (Geyer et al., 2004; Chikita et al., 2021).

RESULTS

ROMS VALIDATION

Due to the lack of in situ measurements during the first six months after the dam rupture, we

extended our hydrodynamic numerical simulation until January 2019, when in situ data were collected. We used hourly time series of current and SSH derived from measurements from three bottom-mounted ADCPs installed along the inner continental shelf (Figure 1). Despite the comparisons between in situ and model-derived data being in a period other than our primary goal, they are still essential to evaluate the model's capability to reproduce important regional shelf processes such as coastal upwelling.

We examined the time variability of the SSH in the three mooring sites (P1, P2, and P3). Comparisons between modeled (red lines in Figure 3) and observed (blue lines in Figure 3) SSH showed good agreement for all mooring sites, with the strongest correlation occurring near
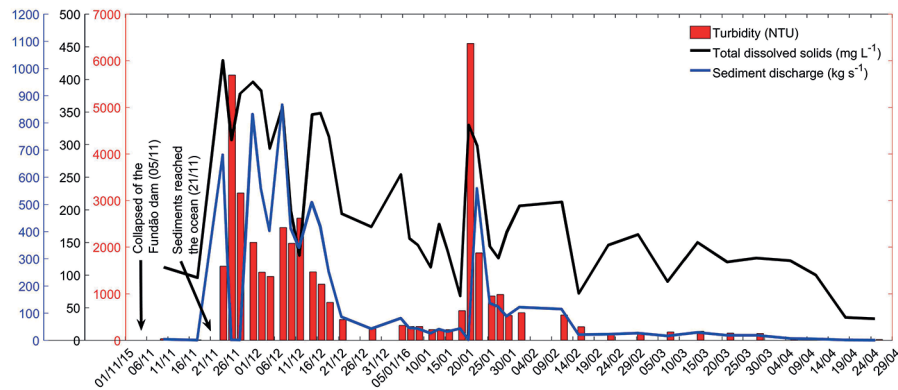

Figure 2. Time series of turbidity (NTU) and total dissolved solids (mg L^{-1}) collected in the Colatina station from November 2015 to April 2016 by the "Companhia de Pesquisa de Recursos Minerais" (CPRM 2015) and the calculated sediment discharge (kg s^{-1}) used in the sediment model.
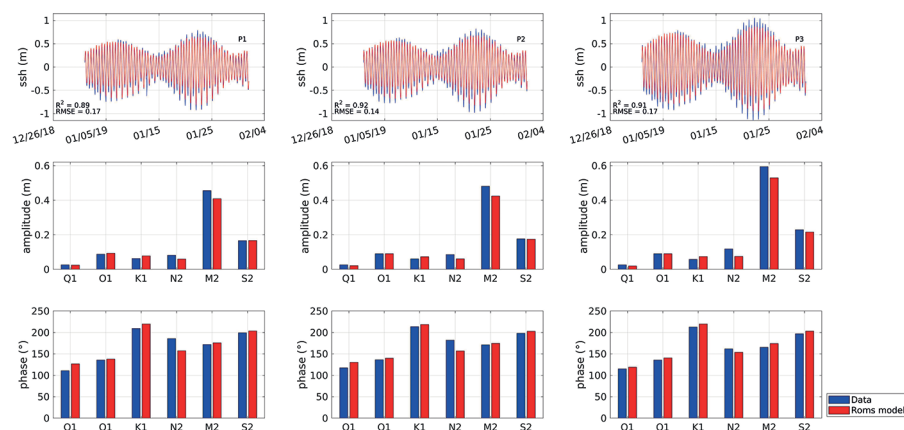

Figure 3. Comparisons between the measured (blue line) and modeled (red line) sea surface height during January 2019. Histograms of amplitude and phase were obtained from harmonic analysis of the measured (blue bars) SSH and simulated (red bars).

the river mouth in P2 (R^2 = 0.92, RMSE = 0.14). These results were similar to those obtained in P1 (R^2 = 0.89, RMSE = 0.17) and P3 (R^2 = 0.91, RMSE = 0.17). In this region, sea-level variability was dominated by tidal fluctuations. Instantaneous differences between modeled and observed SSH during January 2019 (considering astronomical and atmospheric influences) were always smaller than 0.2 m.

Harmonic analysis of the SSH time series revealed that the local tidal regime is semidiurnal with a major contribution of the M_2 constituent. Tidal form numbers (Defant, 1958; Pugh, 1987) were similar for P1 (modeled=0.29, observed=0.24), P2 (modeled=0.27, observed=0.22), and P3 (modeled=0.22, observed=0.18). These values are within the limit of mainly semidiurnal to mixed-semidiurnal tides (Defant, 1958). Comparisons between the modeled (red bars) and the observed (blue bars) amplitude and phase of the principal semidiurnal and diurnal tidal constituents are shown in Figure 3. The results showed good agreement between the numerical results and the data, with differences in the M_2 amplitude of less than 0.07 m.

Considering the 20 days between January 12-31st, 2019, the mean circulation of the continental shelf showed negative (southward) along-shore currents for both the model and observations. However, there was an overestimation of the modeled alongshore velocities obtained in P1 (not shown). For P2 and P3, the fit between the measured and modeled data showed moderate to high correlation, with values of 0.69 to 0.86, respectively (Table 1). Considering the cross-shore velocities, the calculated correlations showed values of 0.42 for P1 and 0.65 for P2, with higher values (0.83) in P3. Basic statistics of the comparisons are shown in Table 1.

To compare subinertial fluctuations of the shelf circulation, low-pass filtered velocity components time series (using a Butterworth digital filter with a cutoff period of 35h) were also investigated (Table 1 - filtered components). Correlation coefficients for both components were nearly the same in P1, although tidal fluctuations were significant to the local circulation variability north of the river mouth (in P2 and P3).

Spectral analysis of the alongshore currents showed that the model could reproduce both the subinertial and supra-inertial processes which were observed on the continental shelf (Figure 4). Supra-inertial fluctuations grow in significance towards the north of the river mouth, at the southern flank of the Abrolhos Bank. Diurnal and semidiurnal peaks were evident in all three mooring sites. However, the semidiurnal band showed higher spectral energy north of the river mouth (P2 and P3). Coherence analysis between winds and currents time series (not shown) revealed that the diurnal band is highly coherent with cross-shore winds, which might be associated with the local sea breeze. At subinertial timescales, cycles between 2-4 days were present for both numerical results and observations (Figure 4). These fluctuations in the shelf circulation were also coherent with the local wind forcing.

SEDIMENT MODEL VERIFICATION

Qualitative validation of the STRiPE sediment model results was done based on MODIS-Aqua and MODIS-Terra 555-nm band images that are indicative of turbid river plumes (Nezlin and DiGiacomo, 2005; Nezlin et al., 2005; Thomas and Weatherbee, 2006; Mendes et al., 2014; Mendes et al., 2017). We identified five different spreading patterns of the DR plume that occurred during the study period (Figure 5). These spreading

Table 1. R^2 and RMSE (m s^{-1}) values between depth-averaged velocity measurements and numerical results in P1, P2 and P3.

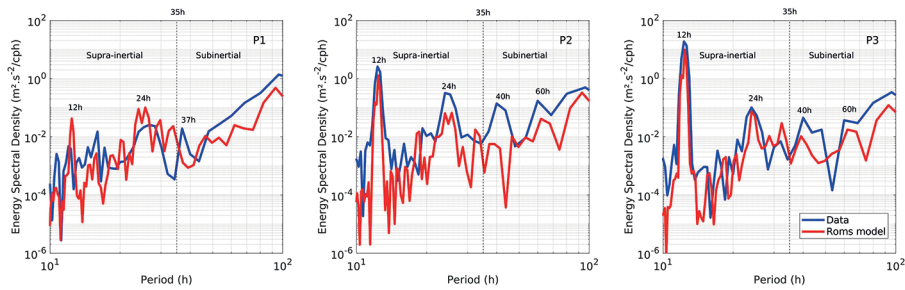| Mooring	Alongshore		Cross-shore		Alongshore filtered		Cross-shore filtered	
	R^2	RMSE	R^2	RMSE	R^2	RMSE	R^2	RMSE
P1	0.14	0.34	0.42	0.05	0.14	0.31	0.39	0.02
P2	0.69	0.09	0.65	0.12	0.41	0.07	0.38	0.01
P3	0.86	0.12	0.83	0.06	0.40	0.02	0.47	0.01

Figure 4. Energy spectra of the along-shore component of the shelf circulation in January 2019 for the three mooring sites (from left to right - P1, P2, and P3). Blue lines denote the observations and red lines the numerical results.
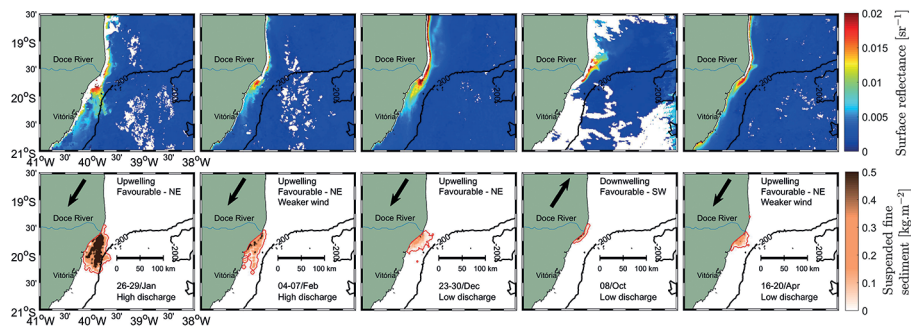

Figure 5. Composites of MODIS-Aqua and MODIS-Terra remote sensing reflectance (sr[-1]) for the 555-nm band (upper panel) and distributions of fine suspended sediment obtained from STRiPE model (lower panel) under five different wind and discharge configurations. Red lines represent the isoline of 0.01 kg m^{-2} sediment concentration. Black arrows indicate the wind direction.

scenarios occurred under particular wind and river discharge configurations. We selected five dates to illustrate these scenarios and compared them to the outputs of the sediment model (Table 2).

The warmer colors (Figure 5, top panel) indicate higher concentrations of suspended material, representing a proxy for the DR plume turbid waters. Under the influence of upwelling favorable winds (Scenario 1) and high river discharge (December 26-29, 2015), the DR plume reached the shelf break, close to 20.3°S (60 km southward from the river mouth). This scenario presented the wider plume dispersion, with the DR plume occupying a large portion of the continental shelf between 19.5°S and 20.5°S. The remote sensing imagery showed similar results, with high turbidity waters advected mostly southward, directly influencing the EPA Costa das Algas.

Weaker upwelling-favorable wind conditions associated with a high river discharge (Scenario 2) reduced the river plume dispersion. As a result, the plume area retracted and remained up to approximately 20°S (about 30 km southward from the river mouth), restricted to the inner shelf.

Low discharge events (Scenarios 3-5) exhibited similar patterns regarding the river plume dispersion. In these conditions, the river plume shrank close to the coast near the river mouth, occupying a smaller area, and did not reach distances greater than 30 km from the source. In addition, under downwelling-favorable wind conditions, the river plume advected northward (less than 40 km), attached to the coast.

DOCE RIVER DISCHARGE AND WIND STRESS FORCING

River discharge climatology (calculated between 1990-2016) shows distinct freshet (November to April) and drought (May to October) periods for the DR runoff, commonly referred to values above and below 600 m³ s⁻¹ (Figure 6 - top panel). DR discharge during freshet periods in 2015 and 2016 was significantly lower than climatological mean values.

Table 2. Scenarios, environmental characteristics, and output dates for the validation of the sediment model between November/2015 and April/2016 (HD = High Discharge, LD = Low Discharge). We included scenario 4 to consider a cloud-free and SW wind condition. The wind data are the results for the location of the green circle in Figure 1.

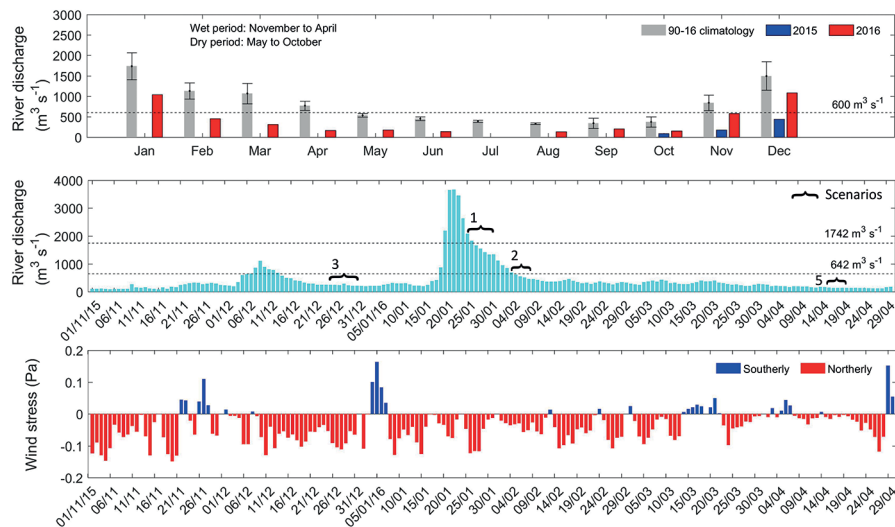| Scenario	Date	River discharge ($m^3 s^{-1}$)	Wind direction	Wind magnitude ($m s^{-1}$)
1	26-29/January/2016	1,606.9 (HD)	Upwelling favorable (NE)	6.8
2	4-7/February/2016	621.8 (HD)	Upwelling favorable (NE - weaker wind)	4.9
3	23-30/December/2015	288.5 (LD)	Upwelling favorable (NE)	6.7
4	8/October/2015	301.1 (LD)	Downwelling favorable (SW)	1.9
5	16-20/April/2016	253.5 (LD)	Upwelling favorable (NE - weaker wind)	3.1

Figure 6. Monthly climatological data from 1990 to 2016 and monthly mean values from 2015 to 2016 of the DR discharge measured at the Colatina city station (no data is available for Jan-Sep 2015) (upper panel). The vertical bars represent the standard error. Middle panel: daily DR discharge measurements from November 2015 to April 2016. The numbers indicate the scenarios dates mentioned in Table 2 (scenario 4 is out of the dates chosen), and the dashed lines mark the discharge limits of the moist conditions in the Doce River, determined from the flow duration curve (FDC) for the period 1990-2013 (Oliveira and Quaresma, 2017). The lower panel shows the vValues of the meridional component of ERA- Interim/ECMWF wind stress meridional component from November 2015 to April 2016 in the study area.

Winds in the study area are predominantly northeasterly, registered over 64% of the time between 2006-2016. However, from November 2015 to April 2016, these winds occurred over 86% of the time (Figure 6), which resulted in the prevailing southward advection of the DR plume.

The highest river discharge was concentrated in January, whereas northeasterly winds occurred during almost the entire period and induced a southward current that transported river-borne sediments toward the EPA Costa das Algas. Nevertheless, between January 4-7,

2016, high turbidity water occurred along the coast up to Abrolhos Marine National Park. This event was associated with the less frequent but moderate to strong southerly winds (Figure 6 - bottom panel) favorable for the northward plume advection. However, the river discharge was very low (~200 $m^3 s^{-1}$), and so was the input of river-borne sediment. According to (Rudorff et al., 2018), the high turbidity of water may result from sediment resuspension due to the action of waves generated by the presence of a subtropical cyclone offshore.

TRANSPORT AND DEPOSITION OF RIVER-BORNE SEDIMENTS

The current pattern induced by the wind forcing associated with the river discharge governed the advection of the DR plume and consequently determined the primary bottom accumulation of river-borne sediments. After six months, the modeled distribution of river-born sediments accumulated at the bottom was highly asymmetrical. Most of it occurred southward of the DR mouth (Figure 7), following the persistence of northeasterly wind stress during the simulated period. The situation is anomalous, probably with more suspended sediments compared to other periods. Northward transport of the plume spreading by southerly winds was infrequent and resulted in a relatively small volume of fine suspended sediments deposited northward of the river mouth (< 5 kg m^{-2}). Sediment accumulated mainly in the inner shelf onshore of the 200 m isobath.

The distribution of fine river-borne surface sediment revealed that the majority of the sediment volume discharged by the river ($> 90\%$) remained in shallow waters (< 20 m) south of the river mouth (Figure 8). A relatively low percentage occurred in the EPA Costa das Algas, while almost no sediment reached Abrolhos Marine National Park. River-borne suspended sediments arrived at the northern part of the EPA Costa das Algas (concentration > 0.01 kg m^{-2}) 40% of the time, but less than 1% reached as far as Abrolhos Marine National Park.

DISCUSSION

The numerical results emphasize the predominance of the wind-driven southward advection in the spreading of river-borne sediments in the marine six months after the environmental disaster. Between November and April, the river discharge is climatologically high (varying from 646 m^3 s^{-1} to 1742 m^3 s^{-1}, Oliveira and Quaresma, 2017). As a result, turbidity within the plume was significantly higher than in the ambient ocean, and the plume was distinctly visible through satellite ocean color
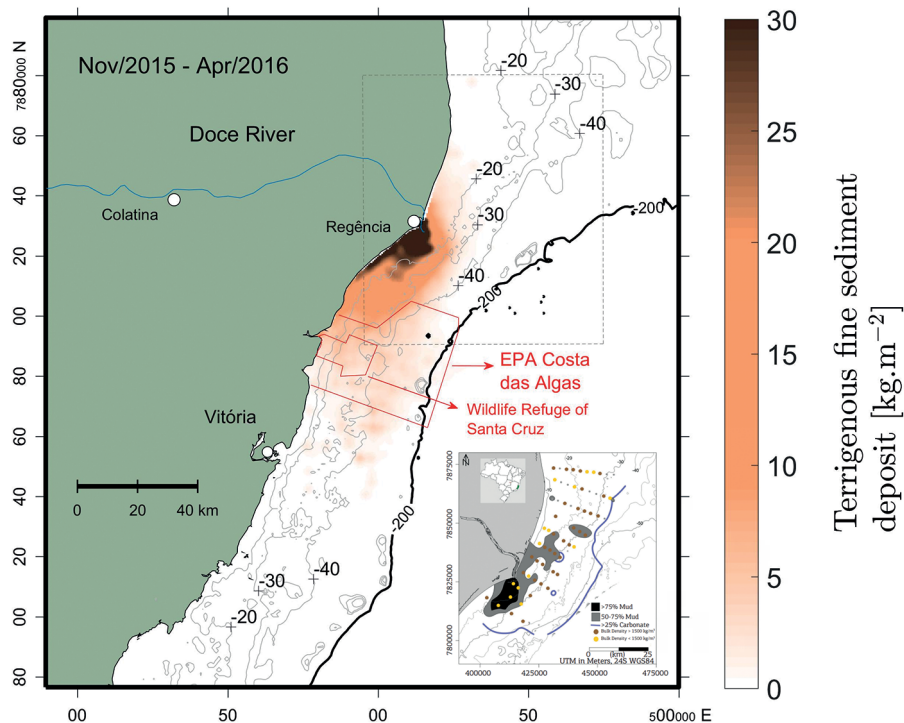

Figure 7. Distribution of fine river-borne sediments deposited at the sea bottom from November 2015 to April 2016. The dashed line highlights where Quaresma et al. (2015) investigated the sediment distribution close to the DR mouth before the disaster (small figure in the right corner).
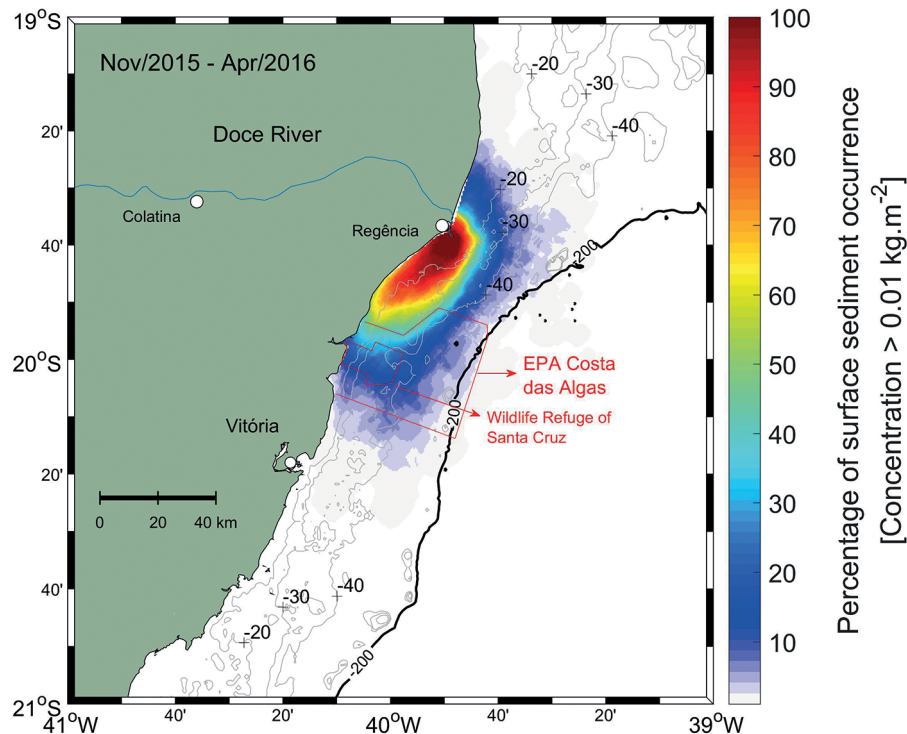
Figure 8. Percentage of occurrence of fine river-borne surface sediment (concentration > 0.01 kg m⁻²) after six months of numerical simulation following the environmental disaster.

composites. Therefore, the DR exhibited high turbidity and sediment discharge concentration during the river flooding period (e.g., January 20-25, 2016) (Figure 2). Nevertheless, the collapse of the Fundão dam increased the river turbidity and total dissolved solids, even during low river discharge conditions, as observed between November 21 and December 6, 2015 (Figure 6), which resulted in more sediment associated with the river plume.

On the other hand, during the low river discharge period (May to October) concentration of suspended sediment in the DR is generally lower. Thus, from ex-situ observations, the low sediment concentration in the plume decreases the visible contrast with the adjacent sea. However, during the dry period, the plume visibility might be affected by intense resuspension of bottom sediment in shallow ocean areas and their subsequent spreading over the shelf by waves, drift currents, and coastal and tidal circulation. This fact hinders accurate identification of the plume spreading extent during the drought season. For instance, Segal et al., 2008, showed that persistent southerly winds and

storm swells might resuspend inner shelf sediments and increase surface water turbidity in the region of the Abrolhos Bank.

Satellite observations suggest that the DR plume's spreading dynamics respond to the river discharge and the local wind stress forcing (and corresponding shelf circulation), which significantly influence the alongshore transport of the river-borne sediment in the surface layer. The sediment discharged from the DR can be transported over tens of kilometers, predominantly southward due to the prevailing northeast winds or, infrequently, northward associated with the passage of cold atmospheric systems in the shelf zone. However, the cross-shore scales of the river plume did not exceed the width of the continental shelf. Therefore, intense cross-shelf transport of river-born sediment is unlikely to occur in the surface layer and is presumed to be governed mainly by the local ocean circulation beneath the surface layer.

During the simulation period, the spreading area of the river-borne sediment did not exceed 75 km from the river mouth in the alongshore direction

and 45 km in the cross-shore far direction (i.e., did not cross the shelf break). This notable alongshore spreading is related to the northeasterly winds that predominate during the wet season (November to April), especially when river discharge is above climatological values. The highest discharge rate observed lasted approximately five days, from January 20-25, 2016, under weak to moderate wind conditions. As a result, river-borne sediments appeared in the coastal region off Vitória city (85 km from the river mouth) for only two days (less than 5% of the simulation period). On the other hand, river-borne sediments spanned almost the whole area of EPA Costa das Algas (~50 km from the river mouth), especially in its shallow water region (< 40 m). These results are consistent with information reported by Bastos et al., 2017, and Rudorff et al., 2018.

Under dominant northeasterly winds, the most turbid inner core of the DR plume was oriented alongshore, extending approximately 11 km south of the river mouth, while the less turbid outer plume reached approximately 39 km (Rudorff et al., 2018). These results found by Rudorff et al., 2018, show good agreement with the spreading pattern of river-borne sediments simulated by the STRiPE model under high river discharge and northeasterly winds conditions. The highest sediment concentration (> 0.5 kg m^{-2}) occurred adjacent to the coastline between the river mouth and the latitude of 19.9°S (January 20-30, 2016). Under lower river discharge conditions, the turbid plume was located adjacent to the river mouth, in an alongshore extension of approximately 15 km.

The most southward region reached by the modeled sediment plume (< 0.01 kg m^{-2}) is close to Vitória city, which is in good accordance with Rudorff et al., 2018, who revealed that the less turbid outer plume was spreading more than 75 km along the southern shelf. Southerly winds arrested the plume near the river mouth (< 8 km), which is also consistent with results presented by Rudorff et al., 2018 (< 5 km).

Infrequently, the DR plume spread northward alongshore from the river mouth, reaching less than 40 km. As a result, only a small concentration (< 0.001 kg m^{-2}) of river-borne sediments reached Abrolhos Marine National Park during a few

events. However, the detailed analysis of the possible environmental impact of these small concentrations of sediment on Abrolhos Marine National Park is beyond the scope of the current study.

The role of wind forcing on the transport of river-borne sediments was identified by satellite imagery. Under the influence of the prevailing north-northeasterly wind stress forcing and high river discharge, the sediment plume propagated southward more than 75 km from the river mouth and occupied a wide area (up to 500 km^2) and remained, for the most part, within the continental shelf. However, during the high discharge period, a small fraction of river-borne sediments were transported off the isobath of 200 m to the deep sea.

Southerly winds, which are also regularly observed in the study region, induced a northward spreading pattern of river-borne sediments (Scenario 4 in Figure 5). Under these conditions, an alongshore geostrophic current was formed, inducing northward sediment transport. The cross-shore scale of this buoyancy current did not exceed 20 km, limiting the river-borne sediment of the surface layer to the shelf area. Low river discharge seems to limit the northward propagation of the river-borne sediments, as was observed on October 8, 2015.

The dependence of river-borne sediment spreading pattern on external forcing conditions can be summarized as follows. Northward propagation of the DR plume occurs under infrequent southerly winds. Its alongshore extent generally does not exceed 40 km. Otherwise, southward plume propagation occurs more often in the absence of, or under northerly, wind forcing and during any discharge conditions, and its propagation can be more than 75 km along the southern shelf (Figure 9).

The deposit of fine sediment simulated in this study (Figure 7) is in good agreement with the results of Quaresma et al., 2015, Bastos et al., 2015 and Bourguignon et al., 2018, based on in situ measurements, which revealed that the finest sediment fraction is transported offshore and deposited mainly southward from the river mouth between 10 m and 30 m isobaths. In contrast, a minor fraction was transported northward along
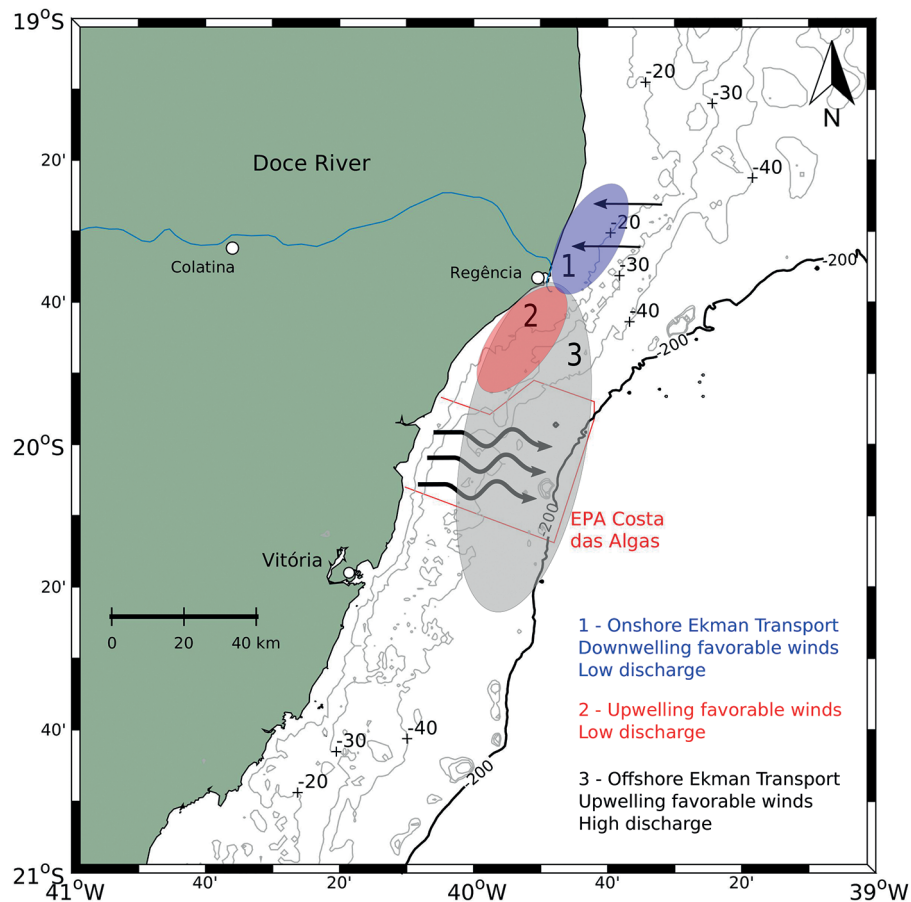
Figure 9. Schematic superficial distribution of the DR sediment under the typical wind and discharge conditions within six months after the environmental disaster. South (north) arrows indicate the main direction of the cross-shore Ekman transport during upwelling (downwelling) favorable winds.

the coast. The simulated bottom sediment distribution was accumulated mostly during northeasterly winds and low river discharge. Therefore, the majority of sediment deposited was close to the shoreline (< 20 m deep), between the river mouth and approximately 20°S. Differently, infrequent southwesterly winds resulted in sediment deposits northward of the DR mouth. The northward extent of the sediment deposit to the seafloor was limited by 19.5°S in the region of the middle shelf, revealing the same pattern and area of terrigenous mud deposit northward of the river mouth observed in the distribution of sedimentary facies (Bastos et al., 2015; Bourguignon et al., 2018).

NUMERICAL LIMITATIONS

The numerical model used in this work does not reproduce bottom resuspension and redeposition

of fine sediment caused by waves and coastal circulation. These processes are significant, especially during the dry period, when the SSH tends to be higher than during the wet season simulated in this study. Despite these limitations, the numerical results agreed with satellite imagery and in situ measurements performed in the study region. Nevertheless, the calculated concentration of fine sediment on the sea surface and seafloor is likely to be different. As a result, the seafloor sediment accumulation area may be larger than estimated by the model.

CONCLUSION

We used Eulerian (ROMS) and Lagrangian (STRiPE) numerical models to reconstruct the river discharge sediment spreading and bottom accumulated in the coastal sea for six months after

the collapse of the Fundão dam on November 5, 2015. The DR plume dynamics and associated transport of river-borne sediment responded to the local wind forcing, ambient circulation, and river discharge rate. The river plume advected predominantly alongshore southward (forced by the north and northeasterly winds) or northward (induced by southerly winds). The former caused local coastal upwelling, in which surface Ekman transport influenced the spreading of the fine sediment offshore. Yet, the cross-shore extent of the river-borne sediments did not exceed the width of the shelf. In addition, infrequent southerly winds arrested the plume near the river mouth resulting in its relatively small alongshore extent. They did not cause intense northward transport of the river-borne suspended sediments.

Most of the fine fraction of the mine slurry accumulated in the vicinity and southward of the river mouth at the inner shelf. River-borne sediment was transported far offshore to the deep ocean only during a few flooding discharge periods. One of the main concerns about the disaster was its possible influence on Abrolhos Marine National Park, the most important coral reef system in Brazil, located 200 km northward of the river mouth. We showed that wind and discharge conditions six months after the disaster hindered the northward spreading of the river plume. As a result, only a small fraction of dissolved and suspended mine tailing waste reached the Abrolhos Marine National Park area. However, no evidence of this event appeared on the seabed. On the other hand, a small fraction of the river-borne sediment near Vitória city could negatively impact local water quality and the marine food web. Future studies should address these questions, including in situ measurements and analysis of contaminants to properly address the potential impact of the environmental disaster in this region.

ACKNOWLEDGMENTS

AUTHOR CONTRIBUTIONS

A.O.: Methodology; Software; Investigation; Writing - original draft;

P.L.F.M.: Supervision; Methodology; Software; Formal Analysis; Investigation; Writing - review & editing;

G.N.M: Formal Analysis; Investigation;

S.F.: Formal Analysis; Investigation;

R.D.G.: Resources; Funding Acquisition; Writing - review & editing.

REFERENCES

ANA (Agência Nacional de Águas). 2016. *Encarte especial sobre a Bacia do Rio Doce - rompimento da barragem em Mariana/MG: conjuntura dos recursos hídricos no Brasil*. Brasília: SPR (Superintendência de Planejamento de Recursos Hídricos), Ministério de Meio Ambiente.

APRILE, F. M., LORANDI, R. & BIANCHINI JUNIOR, I. 2004. A dinâmica costeira e os processos erosivos na foz do Rio Doce, Espírito Santo - Brasil. *Bioikos, PUC-Campinas*, 18(1), 71-78.

ARRUDA, W. Z., CAMPOS, E. J. D., ZHARKOV, V., SOUTELINO, R. G. & SILVEIRA, I. C. A. 2013. Events of equatorward translation of the Vitória Eddy. *Continental Shelf Research*, 70, 61-73.

BASTOS, A. C. 2017. *Monitoramento da Influência da Pluma do Rio Doce após o rompimento da Barragem de Rejeitos em Mariana/MG, Novembro de 2015: processamento, interpretação e consolidação de dados, Vitória, 2017*. Vitória: UFES (Universidade Federal do Espírito Santo).

BASTOS, A. C., MOURA, R. L., AMADO-FILHO, G. M., D'AGOSTINI, D. P., SECCHIN, N. A., FRANCINI-FILHO, R. B., GUTH, A. Z., SUMIDA, P. Y. G., MAHIQUES, M. M. & THOMPSON, F. L. 2013. Buracas: novel and unusual sinkhole-like features in the Abrolhos Bank. *Continental Shelf Research*, 70, 118-125.

BASTOS, A. C., QUARESMA, V. S., MARANGONI, M. B., D'AGOSTINI, D. P., BOURGUIGNON, S. N., CETTO, P. H., SILVA, A. E., AMADO FILHO, G. M., MOURA, R. L. & COLLINS, M. 2015. Shelf morphology as an indicator of sedimentary regimes: a synthesis from a mixed siliciclastic-carbonate shelf on the eastern Brazilian margin. *Journal of South American Earth Sciences*, 63, 125-136.

BERKELMANS, R., JONES, A. & SCHAFFELKE, B. 2012. Salinity thresholds of Acropora spp. on the Great Barrier Reef. *Coral Reefs*, 31(4), 1103-1110.

BEUSEN, A. H. W., DEKKERS, A. L. M., BOUWMAN, A. F., LUDWIG, W. & HARRISON, J. 2005. Estimation of global river transport of sediments and associated particulate C, N, and P. *Global Biogeochemical Cycles*, 19(4), GBS05.

BIANCHINI, A. 2016. *Relatório: avaliação do impacto da lama/pluma Samarco sobre os ambientes costeiros e marinhos (ES e BA) com ênfase nas unidades de conservação. 1ª expedição do navio de pesquisa Soloncy Moura do CEPSUL/ICMBio*. Brasília: Ministério do Meio Ambiente/ICMBio (Instituto Chico Mendes de Conservação da Biodiversidade).

BORGES, A. V. & GYPHENS, N. 2010. Carbonate chemistry in the coastal zone responds more strongly to eutrophication than to ocean acidification. *Limnology and Oceanography*, 55(1), 346-353.

BOURGUIGNON, S. N., BASTOS, A. C., QUARESMA, V. S., VIEIRA, F. V., PINHEIRO, H., AMADO-FILHO, G. M. & MOURA, R. L. 2018. Seabed morphology and sedimentary regimes defining fishing grounds along the Eastern Brazilian Shelf. *Geosciences*, 8(91), 1-17.

BURKE, L., REYTAR, K., SPALDING, M. & PERRY, A. 2011. *Reefs at risk revisited*. Washington, DC: WRI (World Resources Institute).

CARMO, F. F., KAMINO, L. H. Y., JUNIOR, R. T., CAMPOS, I. C., CARMO, F. F., SILVINO, G., CASTRO, K. J. S. X., MAURO, M. L., RODRIGUES, N. U. A., MIRANDA, M. P. S. & PINTO, C. E. F. 2017. Fundão tailings dam failures: the environment tragedy of the largest technological disaster of Brazilian mining in global context. *Perspectives in Ecology and Conservation*, 15(3), 145-151.

CASTELÃO, R. M. & BARTH, J. A. 2006. Upwelling around Cabo Frio, Brazil: the importance of the wind stress curl. *Geophysical Research Letter*, 33(3), L03602, DOI: https://doi.org/10.1029/2005GL025182

CASTRO, B. M. F., BRANDINI, F. P., PIRES-VANIN, A. M. S. & MIRANDA, L. B. 2006. Multidisciplinary oceanographic processes on the Western Atlantic Continental Shelf between 4N and 34S. *In:* ROBINSON, A. R. & BRINK, K. (eds.). *The global coastal ocean*. Cambridge: Harvard University Press.

CASTRO, B. M. F. & MIRANDA, L. B. 1998. Physical oceanography of the western Atlantic continental shelf located between 41°N and 34°S. *In:* ROBINSON, A. R. & BRINK, K. H. (eds.). *The sea*. Oxford: John Wiley and Sons, pp. 209-252.

CHANT, R. J. 2011. Interactions between estuaries and coasts: River plumes their formation, transport, and dispersal. *In:* WOLANSKI, E. & MCLUSKY, D. (eds.). *Treatise on estuarine and coastal science*. Waltham: Academic Press, pp. 213-235, DOI: https://doi.org/10.1016/B978-0-12-374711-2.00209-6

CHIKITA, K. A., WADA, T., KUDO, I., SAITOH, S. & TORATANI, M. 2021. Effects of river discharge and sediment load on sediment plume behaviors in a coastal region: the Yukon River, Alaska and the Bering Sea. *Hydrology*, 8(1), 45, DOI: https://doi.org/10.3390/hydrology8010045

COELHO, A. L. N. 2006. Situação hídrico-geomorfológica da bacia do Rio Doce com base nos dados da série histórica de vazões da Estação de Colatina - ES. *Caminhos de Geografia*, 6(19), 56-79.

COLE, K. & HETLAND, R. D. 2015. The effects of rotation and river discharge on net mixing in small mouth Kelvin number plumes. *Journal of Physical Oceanography*, 46(5), 1421-1436.

COLES, S. L. & JOKIEL, P. 1992. Effects of salinity on coral reefs. *In:* CONNELL, D. W. & HAWKER, D. W. (eds.). *Pollution in tropical aquatic systems*. New York: CRC Press, pp. 147-166.

DEBREU, L. & BLAYO, E. 2008. Two-way embedding algorithms: a review. *Ocean Dynamics*, 58(5-6), 415-428.

DEBREU, L., MARCHESIELLO, P., PENVEN, P. & CAMBON, G. 2012. Two-way nesting in split-explicit ocean models: algorithms, implementation and validation. *Ocean Modeling*, 49-50, 1-21.

DEFANT, A. 1958. *Ebb and flow: the tides of earth, air and water*. Ann Arbor: The University of Michigan Press.

DEE, D. P., UPPALA, S. M., SIMMONS, A. J., BERRISFORD, P., POLI, P., KOBAYASHI, S., ANDRAE, U., BALMASEDA, M. A., BALSAMO, G., BAUER, P., BECHTOLD, P., BELJAARS, A. C. M., VAN DE BERG, L., BIDLOT, J., BORMANN, N., DELSOL, C., DRAGANI, R., FUENTES, M., GEER, A. J., HAIMBERGER, L., HEALY, S. B., HERSBACH, H., HOLM, E. V., ISAKSEN, L., KALLBERG, P., KOHLER, M., MATRICARDI, M., MCNALLY, A. P., MONGE-SANZ, B. M., MORCRETTE, J. J., PARK, B. K., PEUBEY, C., DE ROSNAY, P., TAVOLATO, C., THEPAUT, J. N. & VITART, F. 2011. The ERA-Interim reanalysis: configuration and performance of the data assimilation system. *Quarterly Journal of the Royal Meteorological Society*, 137(656), 553-597, DOI: https://doi.org/10.1002/qj.828

EGBERT, G. D. & EROFEEVA, S. Y. 2002. Efficient inverse modeling of barotropic ocean tides. *Journal of Atmospheric and Oceanic Technology*, 19(2), 183-204.

EKAU, W. 1999. Topographical and hydrographical impacts on macrozooplankton community structure in the Abrolhos Bank region. *Archive of Fishery and Marine Research*, 47(2), 307-320.

ERFTEMEIJER, P. L., RIEGL, B., HOEKSEMA, B. W. & TODD, P. A. 2012. Environmental impacts of dredging and other sediment disturbances on corals: a review. *Marine Pollution Bulletin*, 64(9), 1737-1765.

ESCOBAR, H. 2015. Mud tsunami wreaks ecological havoc in Brazil. *Science*, 350(6265), 1138-1139, DOI: https://doi.org/10.1126/science.350.6265.1138

FABRICIUS, K. E. 2005. Effects of terrestrial runoff on the ecology of corals and coral reefs: review and synthesis. *Marine Pollution Bulletin*, 50(2), 125-146.

FERNANDES, G. W., GOULART, F. F., RANIERI, B. D., COELHO, M. S., DALES, K., BOESCHE, N., BUSTA-MANTE, M., CARVALHO, F. A., CARVALHO, D. C., DIRZO, R., FERNANDES, S., GALETTI JUNIOR, P. M., MILLAN, V. E. G., MIELKE, C., RAMIREZ, J. L., NE-VES, A., ROGASS, C., RIBEIRO, S. P., SCARIOT, A. & SOARES-FILHO, B. 2016. Deep into the mud: eco-logical and socio-economic impacts of the dam breach in Mariana, Brazil. Natureza e Conservação. *Brazilian Journal for Nature Conservation*, 14, 35-45.

FISHER, A. W., NIDZIEKO, N. J., SCULLY, M. E., CHANT, R. J., HUNTER, E. J. & MAZZINI, P. L. F. 2018. Turbu-lent mixing in a far-field plume during the transition to upwelling conditions: microstructure observations from an AUV. *Geophysical Research Letter*, 45(18), 9765-9773, DOI: https://doi.org/10.1029/2018GL078543

FRANCINI-FILHO, R. B., MOURA, R. L., THOMPSON, F. L., REIS, R. M., KAUFMAN, L., KIKUCHI, R. K. P. & LEÃO, Z. M. A. N. 2008. Diseases leading to acce-lerated decline of reef corals in the largest South Atlantic reef complex (Abrolhos Bank, eastern Brazil). *Marine Pollution Bulletin*, 56(5), 1008-1014.

GARVINE, R. W. 1984. Radial spreading of buoyant, sur-face plumes in coastal waters. *Journal of Geophysical Research*, 89(C2), 1989-1996.

GARVINE, R. W. 1995. A dynamical system for classifying buoyant coastal discharges. *Continental Shelf Re-search*, 15(13), 1585-1596.

GEYER, W. R., HILL, P. S., & KINEKE, G. C. 2004. The transport, transformation and dispersal of sediment by buoyant coastal flows. *Continental Shelf Research*, 24, 927-949.

GOMES, L. E. O., CORRÊA, L. B., SÁ, F., NETO, R. R. & BERNARDINO, A. F. 2017. The impacts of the Samar-co mine tailing spill on the Rio Doce estuary, Eastern Brazil. *Marine Pollution Bulletin*, 120(1-2), 28-36, DOI: https://doi.org/10.1016/j.marpolbul.2017.04.056

GUIMARÃES, D. P., REIS, R. J., & LANDAU, E. C. 2010. Índices pluviométricos em Minas Gerais. Sete Lagoas: Embrapa Milho e Sorgo.

HAIDVOGEL, D. B., ARANGO, H., BUDGELL, W. P., COR-NUELLE, B. D., CURCHITSER, E., DILORENZO, E., FENNEL, K., GEYER, W. R., HERMMAN, A. J., LANE-ROLLE, L., LEVIN, J., MCWILLIAMS, J. C., MILLER, A. J., MOORE, A. M., POWELL, T. M., SHCHEPETKIN, A. F., SHERWOOD, C. R., SIGNELL, R. P., WARNER, J. C. & WILKIN, J. 2008. Ocean forecasting in terrain--following coordinates: formulations and skill assesment of the Regional Ocean Modeling System. *Journal of Computational Physics*, 227, 3595-3624.

HATJE, V., PEDREIRA, R. M. A., REZENDE, C. E., SCHET-TINI, C. A. F., SOUZA, G. C., MARIN, D. C. & HACKS-PACHER, P. C. 2017. The environmental impacts of one of the largest tailing dam failures worldwide. *Sci-entific Reports,* 7, 10706, DOI: https://doi.org/10.1038/s41598-017-11143-x

HYCOM (Hybrid Coordinate Ocean Model). 2011. *Consor-tium for data assimilative modeling HYCOM+NCODA Global 1/12º analysis* [online]. Lodz: HYCOM. Available at: http://www.hycom.org/dataserver/glb584analysis/ [Accessed: 2018 Aug 15].

IBAMA (Instituto Brasileiro do Meio Ambiente e dos Recursos Naturais Renováveis). 2006. *Relatório final da proposta de criação das UCs APA Costa das Algas e Revis de Santa Cruz. Volumes I, II, III e IV*. Vitória: IBAMA (Instituto Brasilei-ro do Meio Ambiente e dos Recursos Naturais Renováveis).

IOC (Intergovernmental Oceanographic Commission), IHO (International Hydrographic Organization) & BODC (British Oceanographic Data Centre). 2003. *Centenary edition of the GEBCO digital atlas, published on CD-ROM on be-half of the Intergovernmental Oceanographic Commission and the International Hydrographic Organization as part of the General Bathymetric Chart of the Oceans*. Liverpool: BODC (British Oceanographic Data Centre).

JICKELLS, T. D. 1998. Nutrient biogeochemistry of the coastal zone. *Science*, 281(5374), 217-221.

KOROTENKO, K. A., OSADCHIEV, A. A., ZAVIALOV, P. O., KAO, R. C. & DING, C. F. 2014. Effects of bottom topo-graphy on dynamics of river discharges in tidal regions: case study of twin plumes in Taiwan Strait. *Ocean Sci-ence*, 10, 863-879, DOI: https://os.copernicus.org/arti-cles/10/863/2014/

LARGE, W. G. & POND, S. 1981. Open ocean momentum flux measurements in moderate to strong winds. *Journal of Physical Oceanography*, 11(3), 324-336, DOI: https://doi.org/10.1175/1520-0485(1981)011<0324:OOMFMI>2.0.CO;2

LEÃO, Z. M. A. N. 1999. Abrolhos - o complexo recifal mais extenso do Atlântico Sul. *In:* SCHOBBENHAUS, C., CAMPOS, D. A., QUEIROZ, E. T., WINGE, M. & BERBERT-BORN, M. L. C. (eds.). *Sítios Geológicos e Paleontológicos do Brasil*. Brasília: DNPM/CPRM - Co-missão Brasileira de Sítios Geológicos e Paleobiológi-cos (SIGEP), 2002, v. 1, pp. 345-359.

LEÃO, Z. M. A. N. & KIKUCHI, R. K. P. 2005. A relic coral fauna threatened by global changes and human activities, eas-tern Brazil. *Marine Pollution Bulletin*, 51(5-7), 599-611.

LIMA, K. C., SATYAMURTY, P. & FERNNDEZ, J. P. R. 2010. Large-scale atmospheric conditions associated with heavy rainfall episodes in southeast Brasil. *Theo-retical and Applied Climatology*, 101(1-2), 355-363.

MAGRIS, R. A., MARTA-ALMEIDA, M., MONTEIRO, J. A. F. & BAN, N. C. 2019. A modelling approach to assess the impact of land mining on marine biodiversity: asses-sment in coastal catchments experiencing catastrophic events (SW Brazil). *Science of the Total Environment*, 659, 828-840.

MARTA-ALMEIDA, M., MENDES, R., AMORIM, F. N., CI-RANO, M. & DIAS, J. M. 2016. Fundão Dam collapse: oceanic dispersion of River Doce after the greatest Bra-zilian environmental accident. *Marine Pollution Bulletin*, 112(1-2), 359-364.

MAZZINI, P. L. F. & BARTH, J. A. 2013. A comparison of mechanisms generating vertical transport in the Brazi-lian coastal upwelling regions. *Journal of Geophysical Research: Oceans*, 118, 5977-5993, DOI: https://doi.org/10.1002/2013JC008924

MAZZINI, P. L. F. & CHANT, R. J. 2016. Two-dimensional circulation and mixing in the far field of a surface--advected river plume. *Journal of Geophysical Re-search: Oceans,* 121(6), 3757-3776, DOI: https://doi.org/10.1002/2015JC011059

MAZZINI, P. L. F., CHANT, R. J., SCULLY, M. E., WILKIN, J., HUNTER, E. J. & NIDZIEKO, N. J. 2019. The impact of wind forcing on the thermal wind shear of a river plume. *Journal of Geophysical Research: Oceans*, 124(11), 7908-7925, DOI: https://doi.org/10.1029/2019JC015259

MENDES, R., SALDÍAS, G. S., DECASTRO, M., GÓMEZ-GESTEIRA, M., VAZ, N. & DIAS, J. M. 2017. Seasonal and interannual variability of the Douro turbid river plume, northwestern Iberian Peninsula. *Remote Sensing of Environment,* 401-411.

MENDES, R., VAZ, N., FERNÁNDEZ-NÓVOA, D., SILVA, J. C. B., DECASTRO, M., GÓMEZ-GESTEIRA, M. & DIAS, J. M. 2014. Observation of a turbid plume using MODIS imagery: the case of Douro estuary (Portugal). *Remote Sensing of Environment*, 154, 127-138.

MILLIMAN, J. D. & FARNSWORTH, K. L. 2011. *River discharge to the coastal ocean - a global synthesis*. Cambridge: Cambridge University Press.

MILLIMAN, J. D. & SYVITSKI, J. P. M. 1992. Geomorphic/tectonic control of sediment discharge to the ocean: the importance of small mountainous rivers. *Journal of Geology*, 100(5), 525-544.

MIRANDA, L. B. 1985. Forma da correlação T-S de massas de água das regiões costeira e oceânica entre o Cabo de São Tomé (RJ) e a Ilha de São Sebastião (SP), Brasil. *Boletim do Instituto Oceanográfico*, 33(2), 15-19.

MYERS, N., MITTERMEIER, R. A., MITTERMEIER, C. G., FONSECA, G. A. B. & KENT, J. 2000. Biodiversity hotspots for conservation priorities. *Nature*, 403, 853-858.

NEZLIN, N. P. & DIGIACOMO, P. M. 2005. Satellite ocean color observations of stormwater runoff plumes along the San Pedro Shelf southern California. *Continental Shelf Research*, 25(14), 1692-1711.

NEZLIN, N. P., DIGIACOMO, P. M., STEIN, E. D. & ACKERMAN, D. 2005. Stormwater runoff plumes observed by SeaWiFS radiometer in the Southern California Bight. *Remote Sensing of Environment*, 98(4), 494-510.

OLIVEIRA, K. S. S. & QUARESMA, V. S. 2017. Temporal variability in the suspended sediment load and streamflow of the Doce River. *Journal of South American Earth Sciences*, 78, 101-115.

OSADCHIEV, A. A. 2015. A method for quantifying freshwater discharge rates from satellite observations and Lagrangian numerical modeling of river plumes. *Environmental Research Letters*, 10(8), 085009, DOI: https://doi.org/10.1088/1748-9326/10/8/085009

OSADCHIEV, A. A., KOROTENKO, K. A., ZAVIALOV, P. O., CHIANG, W. S. & LIU, C.C. 2016. Transport and bottom accumulation of fine river sediments under typhoon conditions and associated submarine landslides: case study of the Peinan River, Taiwan. *Natural Hazards and Earth System Sciences*, 16, 41-54, DOI: https://doi.org/10.5194/nhessd-3-5155-2015

OSADCHIEV, A. A. & KORSHENKO, E. 2017. Small river plumes off the northeastern coast of the Black Sea under average climatic and flooding discharge conditions. *Ocean Science*, 13(3), 465-482.

OSADCHIEV, A. A. & SEDAKOV, R. O. 2019. Spreading dynamics of small river plumes off the northeastern coast of the Black Sea observed by Landsat 8 and Sentinel-2. *Remote Sensing of Environment*, 221(2), 522-533.

OSADCHIEV, A. A. & ZAVIALOV, P. O. 2013. Lagrangian model for surface-advected river plume. *Continental Shelf Research*, 58, 96-106, DOI: https://doi.org/10.1016/j.csr.2013.03.010

PETERSON, R. G. & STRAMMA, L. 1991. Upper-level circulation in the south Atlantic Ocean. *Progress in Oceanography*, 26(1), 1-73.

PUGH, D. 1987. *Tides, surges and mean sea level. A handbook for engineers and scientists.* New York: John Wiley and Sons.

QUARESMA, V. S., CATABRIGA, G. M., BOURGUINON, S. C., GODINHO, E. & BASTOS, A. C. 2015. Modern sedimentary processes along the Doce River adjacent continental shelf. *Brazilian Journal of Geology*, 45, 635-644.

RABALAIS, N. N., TURNER, R. E. & SCAVIA, D. 2002. Beyond science into policy: Gulf of Mexico hypoxia and the Mississippi River. *BioScience*, 52(2), 129-142.

REIFEL, K. M., JOHNSON, S. C., DIGIACOMO, P. M., MENGEL, M. J., NEZLIN, N. P., WARRICK, J. A. & JONES, B. H. 2009. Impacts of stormwater runoff in the Southern California Bight: relationships among plume constituents. *Continental Shelf Research*, 29(15), 1821-1835.

RODRIGUES, R. R. & LORENZZETTI, J. A. 2001. A numerical study of the effects of bottom topography and coastline geometry on the South-East Brazilian coastal upwelling. *Continental Shelf Research*, 21(4), 371-349.

RUDORFF, N., RUDORFF, C. M., KAMPEL, M. & ORTIZ, G. 2018. Remote sensing monitoring of the impact of a major mining wastewater disaster on the turbidity of the Doce River plume off the eastern Brazilian coast. *ISPRS Journal of Photogrammetry and Remote Sensing*, 145, 349-361.

SAMARCO. 2016. *Atualização do plano de recuperação ambiental integrado*. Belo Horizonte: SAMARCO.

SEGAL, B., EVANGELISTA, H., KAMPEL, M., GONÇALVES, A. C., POLITO, P. S. & SANTOS, E. A. 2008. Potential impacts of polar fronts on sedimentation processes at Abrolhos coral reef (South-West Atlantic Ocean/Brazil). *Continental Shelf Research*, 28(4-5), 533-544.

SEGURA, F., NUNES, E. A., PANIZ, F., PANIZ, F. P., PAULELLI, A. C. C., RODRIGUES, G. B., BRAGA, G. U. L., PEDREIRA FILHO, W. R., BARBOSA JÚNIOR, F., CARCHIARO, G., SILVA, F. F. & BATISTA, B. L. 2016. Potential risks of the residue from Samarco's mine dam burst (Bento Rodrigues, Brazil). *Environmental Pollution*, 218, 813-825.

SGB (Serviço Geológico do Brasil - CPRM). 2015. *Sistema de alerta de eventos críticos da bacia hidrográfica do Rio Doce* [online]. Rio de Janeiro: SGB, pp. 147-166. Available at: https://www.cprm.gov.br/sace/index_bacias_monitoradas.php [Accessed: 2016 Jun 20].

SHCHEPETKIN, A. F. & MCWILLIAMS, J. C. 2005. The regional oceanic modeling system (ROMS): a split-explicit, free-surface, topography-following-coordinate oceanic model. *Ocean Modelling*, 9(4), 347-404.

SNIRH (Sistema Nacional de Informação de Recursos Hídricos). 2017. *Portal Hidroweb* [online]. Brasil: SNIRH. Available at: http://www.snirh.gov.br/hidroweb/ [Accessed: 2017 Apr 03].

SOUTELINO, R. G., GANGOPADHYAY, A. & SILVEIRA, I. C. A. 2013. The roles of vertical shear and topography on the eddy formation near the site of origin of the Brazil Current. *Continental Shelf Research*, 70, 46-60.

STRAMMA, L. & ENGLAND, M. 1999. On the water masses and mean circulation of the South Atlantic Ocean. *Journal of Geophysical Research*, 104(C9), 20863-20883.

THOMAS, A. C. & WEATHERBEE, R. A. 2006. Satellite--measured temporal variability of the Columbia River plume. *Remote Sensing of Environment*, 100, 167-178.

WANG, B. 2006. Cultural eutrophication in the Changjian (Yangtze River) plume: history and perspective. *Estuarine, Coastal and Shelf Science*, 69(3-4), 471-477.

WEN, L., SHILLER, A., SANTSCHI, P. & GILL, G. 1999. Trace element behavior in Gulf of Mexico estuaries. *In:* BIANCHI, T. S., PENNOCK, J. R. & TWILLEY, R. R. (eds.). *Biogeochemistry of Gulf of Mexico Estuaries*. New York: John Wiley and Sons, pp. 303-346.

WRIGHT, L. D. 1977. Sediment transport and deposition at river mouths: a synthesis. *Geological Society of America Bulletin*, 88(6), 857-868.